Acta Geotechnica (2006) 1:15–27
DOI 10.1007/s11440-005-0003-3

RESEARCH PAPER

A simple hypoplastic model for normally consolidated clay

Wen-Xiong Huang · Wei Wu · De-An Sun · Scott Sloan

Received: 31 August 2005 / Accepted: 14 October 2005 / Published online: 22 April 2006

Abstract The paper presents a simple constitutive model for normally consolidated clay. A mathematical formulation, using a single tensor-valued function to define the incrementally nonlinear stress–strain relation, is proposed based on the basic concept of hypoplasticity. The structure of the tensor-valued function is determined in the light of the response envelope. Particular attention is paid towards incorporating the critical state and to the capability for capturing undrained behaviour of clayey soils. With five material parameters that can be determined easily from isotropic consolidation and triaxial compression tests, the model is shown to provide good predictions for the response of normally consolidated clay along various stress paths, including drained true triaxial tests and undrained shear tests.

Keywords Constitutive model · Normally consolidated clay · Hypoplasticity

1. Introduction

Constitutive models for soil can be developed by following either the geometrical or algebraical approach [25]. The former is based on plasticity theory with its plastic potential and flow rule, while the latter is based on nonlinear tensorial functions. The prominent representatives of these two approaches are the critical state model and the hypoplastic model.

The critical state model in its simplest form contains four material parameters and is primarily applicable to normally consolidated clay, hence the synonym Cam-clay. The development of Cam-clay for sand, Granta-gravel [18] was less successful. Indeed, the behaviour of dense sand in drained tests and of loose sand in undrained tests cannot be reproduced properly by this simple model. Recently, some modified critical state models based on a state parameter [3] have been proposed for sand [28, 11, 27].

The hypoplastic model in its simplest form also contains four parameters, but is primarily applicable to sand. There are numerous hypoplastic models in the literature, which have been developed mainly for sands [24, 7, 5]. Readers can refer to Kolymbas [10] for an outline of the theory of hypoplasticity. A review of the development in hypoplastic modelling of granular materials can be found in Wu and Kolymbas [26] and Tamagnini et al. [19]. The application of the hypoplastic approach to clay has been less successful. The effective stress paths in undrained triaxial tests form a vertex on the diagonal of principal stress space, which is reminiscent of the bullet-shaped yield surface used in the Granta-gravel formulation. Moreover, the model shows rather poor performance for loading reversals. Recently, a hypoplastic model for clay was proposed by Mašín [12] based on a formulation suggested by Niemunis [16]. While this model can capture many important features of clayey soils, it also suffers from poor performance in undrained condition. Simulations indicate that its effective stress predictions for undrained tests are unrealistic.

In this paper, a simple hypoplastic model for clayey soil is presented. Starting from a basic formulation, the model focuses on a better representation of the response of normally consolidated clay to loading and unloading along

W.-X. Huang · D.-A. Sun · S. Sloan
School of Engineering, The University of Newcastle, Callaghan, Australia

W. Wu (✉)
Institut für Geotechnik, Universität für Bodenkultur, Feistmantelstr. 4, 1180 Vienna, Austria
E-mail: wei.wu@boku.ac.at

various stress paths. Emphasis is given to the improvement of the predictions of model under undrained conditions. The performance of the proposed model is compared with experimental data for normally consolidated clay obtained from drained and undrained tests along various stress paths. It is shown that the model is suitable for describing the rate-independent behaviour of normally consolidated clay under loading and unloading for medium to large strains. Some improvement, however, is necessary for predicting soil response under very small strains. Further modification may be made in this area following Niemunis and Herle [15] and Niemunis [16] to incorporate the concept of intergranular strain.

In the following, except where specified otherwise, effective stress is used in the sense of Terzaghi's effective stress principle. The Cauchy stress tensor, denoted as $\boldsymbol{\sigma}$, is used with a power conjugated strain rate, denoted as $\dot{\boldsymbol{\varepsilon}}$, which is the symmetric part of the velocity gradient of the continuum.

2. General framework

A hypoplasticity model can be regarded as a generalisation of a hypoelastic constitutive relation first discussed by Truesdell [20], where the stress rate $\dot{\boldsymbol{\sigma}}$ in response to material deformation is expressed as a nonlinear tensor-valued function of Cauchy stress $\boldsymbol{\sigma}$, strain rate $\dot{\boldsymbol{\varepsilon}}$ and some other internal variables $\boldsymbol{q}$. A general form for describing rate-independent material behaviour can be written as [23]

$$\dot{\boldsymbol{\sigma}} = \mathbf{L}(\boldsymbol{\sigma},\boldsymbol{q}) : \dot{\boldsymbol{\varepsilon}} + \boldsymbol{N}(\boldsymbol{\sigma},\boldsymbol{q})\|\dot{\boldsymbol{\varepsilon}}\| = \mathbf{L} : (\dot{\boldsymbol{\varepsilon}} - \boldsymbol{B}\|\dot{\boldsymbol{\varepsilon}}\|). \tag{1}$$

Here $\mathbf{L}$ represents a fourth order tensor and $\boldsymbol{N}$ and $\boldsymbol{B}$ represent second order tensors. $\boldsymbol{N}$ and $\boldsymbol{B}$ are related to one another via $\boldsymbol{B}=-\mathbf{L}^{-1}:\boldsymbol{N}$. In this paper, a Euclidean norm is used for a second order tensor $\boldsymbol{A}$ as $\|\boldsymbol{A}\| = \sqrt{\boldsymbol{A} : \boldsymbol{A}}$, while $\|\dot{\boldsymbol{\varepsilon}}\| = \sqrt{\dot{\boldsymbol{\varepsilon}} : \dot{\boldsymbol{\varepsilon}}}$ is the Euclidean norm of the strain rate and $\vec{\dot{\boldsymbol{\varepsilon}}} = \dot{\boldsymbol{\varepsilon}}/\|\dot{\boldsymbol{\varepsilon}}\|$ defines the direction of the strain rate. Obviously, the tangential material stiffness described by this equation is $(\mathbf{L} + \boldsymbol{N} \otimes \vec{\dot{\boldsymbol{\varepsilon}}})$, which depends not only on the state variables $\boldsymbol{\sigma}$ and $\boldsymbol{q}$, but also on the direction of the strain rate $\vec{\dot{\boldsymbol{\varepsilon}}}$. Varying directional stiffness is clearly modelled by this single equation.

To provide some insight into the structure of Eq. 1, a geometrical interpretation is presented using the so-called response envelope introduced by Gudehus [6]. The response envelope is given as the stress rate responses to all strain rate inputs of unit magnitude. The length of a stress rate response vector in the principal stress rate space represents the directional material stiffness defined by Eq. 1. The first part in Eq. 1, which is linear in $\dot{\boldsymbol{\varepsilon}}$, defines stress rate responses forming an ellipsoid in the principal stress rate space, as schematically shown by the dashed ellipse in a 2D plot in Fig. 1(b). The second part in Eq. 1, which is nonlinear in $\dot{\boldsymbol{\varepsilon}}$, defines a translation of the response ellipsoid as represented by the vector $\overline{cc'}$. The overall stress rate response is an ellipsoid as represented by the solid ellipse in Fig. 1(b). Apparently, the tangential material stiffness represented by the length of the response stress rate vectors in Fig. 1(b) varies continuously with the direction of the strain rate. The response envelope of stress increments with respect to strain increment can also be plotted in the principal stress space as given in Fig. 1(c), which demonstrates the variation of directional stiffness with the change of stress state.

Equation 1 describes a steady flow state for continuing deformation when the directional stiffness vanishes (the point marked with a strain rate in Fig. 1c). At a steady flowing state, we have $\dot{\boldsymbol{\sigma}} = \mathbf{0}$, which corresponds to $\vec{\dot{\boldsymbol{\varepsilon}}}^{\mathrm{f}} = \boldsymbol{B}^{\mathrm{f}} = -\mathbf{L}^{-1} : \boldsymbol{N}(\boldsymbol{\sigma}^{\mathrm{f}}, \boldsymbol{q}^{\mathrm{f}})$. Therefore the direction of the strain rate is determined by tensor $\boldsymbol{B}$. The limit condition satisfied by stress and other state variables at a steady flow state is then described by

$$\left\|\boldsymbol{B}^{\mathrm{f}}\right\| - 1 = 0. \tag{2}$$

In order to incorporate the critical state for soils [18, 17], the formulation should enforce a vanishing volumetric

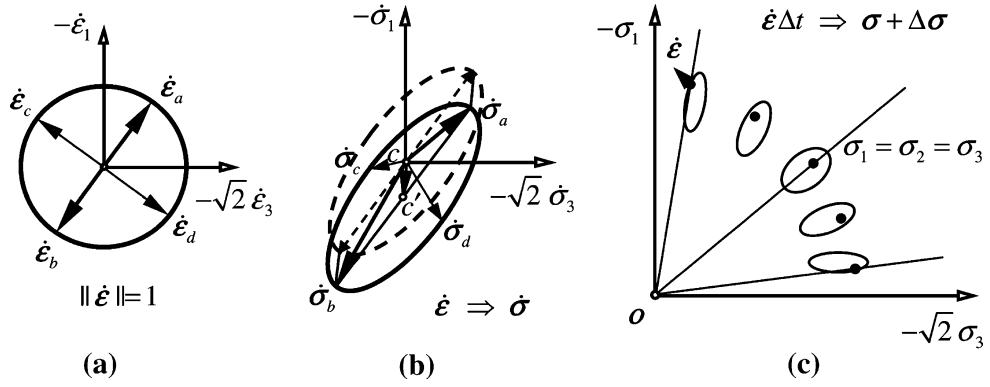

Fig. 1 Schematic representation of response envelope of Eq. 1

deformation at a flowing state. This requirement can be represented by the following condition:

$$\operatorname{tr} \boldsymbol{B}^{\mathrm{f}} = \operatorname{tr} \vec{\dot{\boldsymbol{\varepsilon}}}^{\mathrm{f}} = 0. \tag{3}$$

3. A basic formulation

We start our discussion with a hypoplastic equation of the form:

$$\dot{\boldsymbol{\sigma}} = \chi_1 (p/p_{\mathrm{r}})^m [\hat{a}^2 \dot{\boldsymbol{\varepsilon}} + \hat{\boldsymbol{\sigma}}(\hat{\boldsymbol{\sigma}} : \dot{\boldsymbol{\varepsilon}}) + \hat{a}(\hat{\boldsymbol{\sigma}} + \hat{\boldsymbol{\sigma}}_{\mathrm{d}}) \|\dot{\boldsymbol{\varepsilon}}\|], \tag{4}$$

which is a basic version of the constitutive model proposed for sands by Gudehus [7] and Bauer [1]. This equation sets $\mathbf{L} = \chi_1 (p/p_{\mathrm{r}})^m (\hat{a}^2 \mathbf{I} + \hat{\boldsymbol{\sigma}} \otimes \hat{\boldsymbol{\sigma}})$ and $\boldsymbol{N} = \chi_1 (p/p_{\mathrm{r}})^m \hat{a} (\hat{\boldsymbol{\sigma}} + \hat{\boldsymbol{\sigma}}_{\mathrm{d}})$, where $p = \operatorname{tr} \boldsymbol{\sigma}/3$ is the mean pressure and p_{r} a reference pressure, $\mathbf{I}$ represents the unit tensor of order four, $\hat{\boldsymbol{\sigma}} = \boldsymbol{\sigma}/\operatorname{tr}\boldsymbol{\sigma}$ is the normalized stress and $\hat{\boldsymbol{\sigma}}_{\mathrm{d}} = \hat{\boldsymbol{\sigma}} - \mathbf{1}/3$ is its deviator. The quantity p_{r} denotes a reference pressure, while m is a parameter describing the degree of pressure dependence of the tangential material stiffness, which can be determined together with the factor χ_1 from a soil compression law as discussed in the following section. $\hat{a}$ is a parameter related to the limit stress at steady flow state.

This simple constitutive equation has some nice properties, including sweep-out-memory (SOM) properties under proportional loading [9], and strain-hardening behaviour with a contractive volumetric strain for shear tests. It, therefore, captures, at least qualitatively, the basic features of normally consolidated clays. Moreover, the critical state concept is incorporated in this equation in such a way that the volumetric deformation vanishes when a steady flow state is approached. To show this, we examine an explicit expression for the second order tensor $\boldsymbol{B} = -\mathbf{L}^{-1} : \boldsymbol{N}$ which is

$$\boldsymbol{B} = -\frac{1}{\hat{a}} \left(\frac{\hat{a}^2 - \|\hat{\boldsymbol{\sigma}}_{\mathrm{d}}\|^2}{\hat{a}^2 + \|\hat{\boldsymbol{\sigma}}\|^2} \hat{\boldsymbol{\sigma}} + \hat{\boldsymbol{\sigma}}_{\mathrm{d}} \right). \tag{5}$$

It can be shown that $\|\boldsymbol{B}\|$ increases monotonically with $\|\hat{\boldsymbol{\sigma}}_{\mathrm{d}}\| \in [0, \hat{a}]$. The limit condition 2 is satisfied for

$$\|\hat{\boldsymbol{\sigma}}_{\mathrm{d}}\| = \|\hat{\boldsymbol{\sigma}}_{\mathrm{d}}^{\mathrm{f}}\| = \hat{a}, \tag{6}$$

with $\boldsymbol{B} = \boldsymbol{B}^{\mathrm{f}} = -\hat{\boldsymbol{\sigma}}_{\mathrm{d}}^{\mathrm{f}}/\hat{a}$. Since condition 3 is fulfilled simultaneously, the critical state is described concisely by the formulation 4.

We note that the parameter $\hat{a}$ in this formulation is related to the limit value of the normalized deviatoric stress $\|\hat{\boldsymbol{\sigma}}_{\mathrm{d}}\|$. With a constant $\hat{a}$, Eq. 6 represents a conical surface in the principal stress space, which corresponds to a Drucker–Prager type limit stress condition. Other limit stress conditions can be incorporated into this model by a relevant interpolation for $\hat{a}$ as discussed in detail by Bauer [2]. In the present work, $\hat{a}$ takes the following representation, which incorporates the Matsuoka–Nakai limit condition [2, 21]:

$$\hat{a} = \hat{a}_i \left(\sqrt{\frac{3}{8}\|\hat{\boldsymbol{\sigma}}_{\mathrm{d}}\|^2 + \left(1 - \frac{3}{2}\|\hat{\boldsymbol{\sigma}}_{\mathrm{d}}\|^2\right) \Big/ \left(1 - \sqrt{\frac{3}{2}}\|\hat{\boldsymbol{\sigma}}_{\mathrm{d}}\| \cos(3\theta)\right)} + \sqrt{\frac{3}{8}}\|\hat{\boldsymbol{\sigma}}_{\mathrm{d}}\| \right). \tag{7}$$

Here θ is the Lode angle (Fig. 2) defined by $\cos(3\theta) = \sqrt{6} \operatorname{tr} \hat{\boldsymbol{\sigma}}_{\mathrm{d}}^3 / \|\hat{\boldsymbol{\sigma}}_{\mathrm{d}}\|^3$, and $\hat{a}_i$ represents the value of $\hat{a}$ at an isotropic stress state which is related to the critical friction angle φ_{c} according to

$$\hat{a}_i = \sqrt{\frac{8}{3}} \frac{\sin \varphi_{\mathrm{c}}}{3 + \sin \varphi_{\mathrm{c}}}. \tag{8}$$

4. Barotropy and pyknotropy

Barotropy and pyknotropy refer to the pressure and density dependency of soil behaviour. For granular soils, the stress response to a strain input depends explicitly on density, and the tangential stiffness depends on pressure in a way which is weaker than linear [7]. For clayey soil, a linear pressure dependency of the tangential stiffness is widely accepted to be a good approximation of real soil behaviour. For normally consolidated remoulded clay, the pyknotropy factor can be neglected.

It is widely accepted that, under isotropic compression and unloading, a normally consolidated clay can be described by the following linear $e - \ln p$ relations:

$$e = e_0 - \lambda \ln(p/p_0) \quad \text{for loading.} \tag{9a}$$

$$e = e_1 - \kappa \ln(p/p_1) \quad \text{for unloading.} \tag{9b}$$

Here λ and κ are the compression and swelling indices in a natural-logarithmic coordinate system, and represent the compressibility and swelling behaviour of soil. Another popular compression/swelling law for clayey soils defines a linear relation between the logarithmic specific volume (v=1+e) and the logarithmic mean pressure according to

$$\ln\left(\frac{1+e}{1+e_0}\right) = -\lambda^* \ln(p/p_0) \quad \text{for loading.} \tag{10a}$$

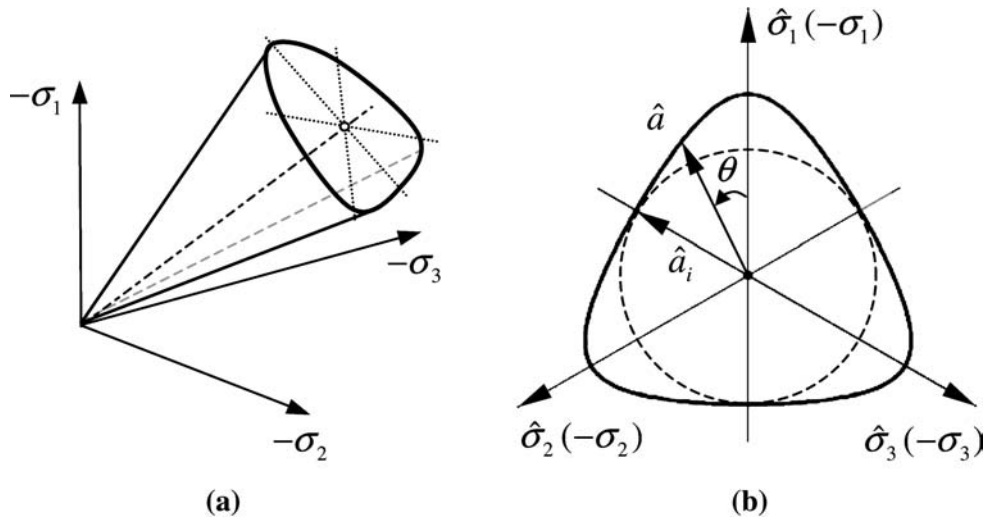

Fig. 2 Limit stress surface: **a** in the principal stress space and **b** in the deviatoric stress plane

$$\ln\left(\frac{1+e}{1+e_1}\right) = -\kappa^* \ln(p/p_1) \quad \text{for unloading.} \tag{10b}$$

Here p_0 and p_1 represent pressures at the beginning of loading and unloading, respectively, with e_0 and e_1 being the corresponding void ratios. The parameters λ^* and κ^* are counterparts of λ and κ in a double-logarithmic coordinate system and can be used to fit the same test data. For many stress ranges that occur in practice, the difference between Eqs. 9a, b and 10a, b is insignificant.

For Eq. 4 to be consistent with Eq. 9a or Eq. 10a, we need only to set m=1 and χ_1 to one of the following expressions, respectively:

$$\chi_1 = \frac{3(1+e)p_r}{\lambda\left(\hat{a}_0^2 + \frac{1}{3} - \frac{1}{\sqrt{3}}\hat{a}_0\right)}, \tag{11}$$

$$\chi_1 = \frac{3p_r}{\lambda^*\left(\hat{a}_0^2 + \frac{1}{3} - \frac{1}{\sqrt{3}}\hat{a}_0\right)}. \tag{12}$$

To show this, we can write Eq. 4 for an isotropic compression test in the form:

$$\begin{aligned} -3\dot{p} &= \chi_1 (p/p_r)^m \left(\hat{a}_i^2 + \frac{1}{3} - \frac{1}{\sqrt{3}}\hat{a}_i\right)\dot{\varepsilon}_v \\ &= \chi_1 (p/p_r)^m \left(\hat{a}_i^2 + \frac{1}{3} - \frac{1}{\sqrt{3}}\hat{a}_i\right)\frac{\dot{e}}{1+e}. \end{aligned} \tag{13}$$

Here $\dot{\varepsilon}_v = \mathrm{tr}\dot{\boldsymbol{\varepsilon}}$ denotes the volumetric strain rate and $p = -\mathrm{tr}\boldsymbol{\sigma}/3$ the mean pressure. The volumetric strain rate is related to the void ratio rate by $\dot{e} = (1+e)\,\dot{\varepsilon}_v$. The above results are obtained by comparing Eq. 13 with the rate relation between the void ratio e and mean pressure p defined by Eqs. 9a and 10a, that is, $\dot{e} = -\lambda\dot{p}/p$ and $\dot{e} = -\lambda^*(1+e)\dot{p}/p$.

5. Proposed formulation

With only two parameters, the basic formulation of Eq. 4 is not adequate for capturing the stress–strain response and volume change behaviour quantitatively. Besides, it has the key shortcoming that its predictions for undrained loading are unrealistic. Another deficiency is that the directional stiffness is not adjustable, so that the differences between loading/unloading and isotropic compression/shear cannot be modelled. The latter has been discussed by Herle and Kolymbas [8]. A geometrical illustration for an isotropic state is presented in Fig. 3b. The following proposed model aims to overcome these shortcomings.

The proposed model takes the following form:

$$\dot{\boldsymbol{\sigma}} = f_s[\hat{a}^2\dot{\boldsymbol{\varepsilon}} + \chi_2\hat{\boldsymbol{\sigma}}(\hat{\boldsymbol{\sigma}}:\dot{\boldsymbol{\varepsilon}}) + \chi_3\hat{\boldsymbol{\sigma}} < \hat{\boldsymbol{\sigma}}:\dot{\boldsymbol{\varepsilon}} > + \hat{a}\,(\chi_3\hat{\boldsymbol{\sigma}} + 2\hat{\boldsymbol{\sigma}}_d)\|\dot{\boldsymbol{\varepsilon}}\|]. \tag{14}$$

where the factors χ_2, χ_3 and χ_4 are included to introduce some flexibility to the model. The term $<\hat{\boldsymbol{\sigma}}:\dot{\boldsymbol{\varepsilon}}>$ has the following representation:

$$<\hat{\boldsymbol{\sigma}}:\dot{\boldsymbol{\varepsilon}}> = \begin{cases} \hat{\boldsymbol{\sigma}}:\dot{\boldsymbol{\varepsilon}} & \text{for } \hat{\boldsymbol{\sigma}}:\dot{\boldsymbol{\varepsilon}} > 0, \\ 0 & \text{for } \hat{\boldsymbol{\sigma}}:\dot{\boldsymbol{\varepsilon}} \leqslant 0. \end{cases} \tag{15}$$

This term is introduced to model the directional stiffness for unloading, as it is activated only for $\boldsymbol{\sigma}:\dot{\boldsymbol{\varepsilon}}<0$ (note that we have a factor $\mathrm{tr}\boldsymbol{\sigma}<0$ in $\hat{\boldsymbol{\sigma}}$). The stiffness factor f_s in Eq. 14 takes a form which is consistent with the isotropic compression law 10a:

$$f_s = \frac{3(1+e)p}{\lambda\left(\hat{a}_i^2 + \frac{1}{3}\chi_{2i} - \frac{1}{\sqrt{3}}\hat{a}_i\chi_{4i}\right)}. \tag{16}$$

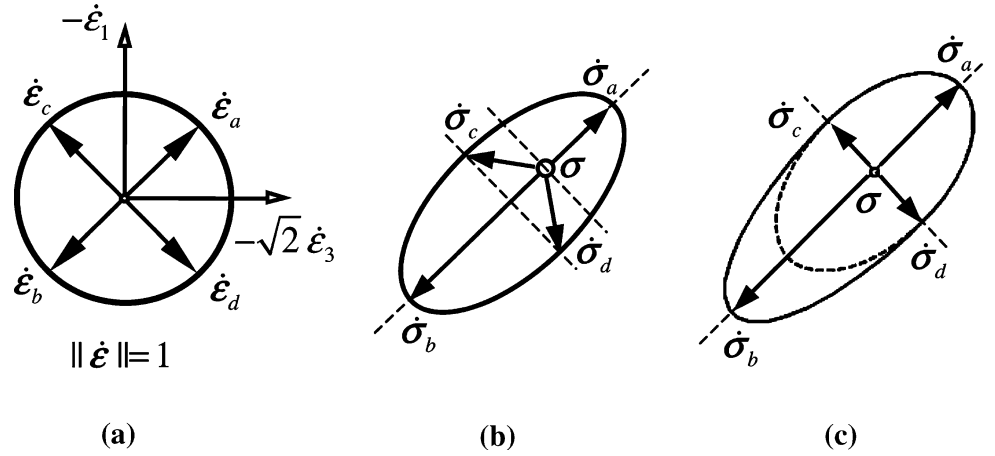

Fig. 3 Response envelope under isotropic stress: **a** input of strain rate of unit magnitude, **b** response envelope of formulation 4 and **c** response envelope of formulation 14

Here χ_{2i} and χ_{4i} denote, respectively, the values of factors χ_2 and χ_4 at an isotropic state for $\|\hat{\boldsymbol{\sigma}}_\mathrm{d}\| = 0$.

In the following, we consider the values for χ_2, χ_3 and χ_4 at an isotropic state and at a steady flow state. Values for these factors at other stress states are then determined by interpolation.

With respect to an elementary test with $\hat{\boldsymbol{\sigma}} : \dot{\boldsymbol{\varepsilon}} \geq 0$, we can write Eq. 16 in the decomposed form:

$$-\dot{p} = \frac{1}{3} f_\mathrm{s} \left[\left(\hat{a}^2 + \frac{1}{3}\eta_2 \right) \dot{\varepsilon}_\mathrm{v} + \chi_2 \, \hat{\boldsymbol{\sigma}}_\mathrm{d} : \dot{\boldsymbol{\varepsilon}}_\mathrm{d} + \chi_4 \hat{a} \sqrt{\frac{1}{3}\dot{\varepsilon}_\mathrm{v}^2 + \dot{\boldsymbol{\varepsilon}}_\mathrm{d} : \dot{\boldsymbol{\varepsilon}}_\mathrm{d}} \right], \tag{17a}$$

$$\dot{\boldsymbol{\sigma}}_\mathrm{d} = f_\mathrm{s} \left[\hat{a}^2 \dot{\boldsymbol{\varepsilon}}_\mathrm{d} + \chi_2 \left(\frac{1}{3}\dot{\varepsilon}_\mathrm{v} + \hat{\boldsymbol{\sigma}}_\mathrm{d} : \dot{\boldsymbol{\varepsilon}}_\mathrm{d} \right) \hat{\boldsymbol{\sigma}}_\mathrm{d} + (1+\chi_4)\hat{a}\hat{\boldsymbol{\sigma}}_\mathrm{d} \sqrt{\frac{1}{3}\dot{\varepsilon}_\mathrm{v}^2 + \dot{\boldsymbol{\varepsilon}}_\mathrm{d} : \dot{\boldsymbol{\varepsilon}}_\mathrm{d}} \right]. \tag{17b}$$

where $\dot{\boldsymbol{\varepsilon}}_\mathrm{d} = \dot{\boldsymbol{\varepsilon}} - \dot{\varepsilon}_\mathrm{v}\,\mathbf{1}/3$ represents the deviatoric strain rate. Starting from an isotropic stress state, we have initially

$$-\dot{p}_i = \frac{1}{3} f_\mathrm{s} \left[\left(\hat{a}_i^2 + \frac{1}{3}\chi_{2i} \right) \dot{\varepsilon}_\mathrm{v} + \chi_{4i} \hat{a}_i \sqrt{\frac{1}{3}\dot{\varepsilon}_\mathrm{v}^2 + \dot{\boldsymbol{\varepsilon}}_\mathrm{d} : \dot{\boldsymbol{\varepsilon}}_\mathrm{d}} \right]$$

and $\hat{\boldsymbol{\sigma}}_\mathrm{d} = \mathbf{0}$. Let us consider first an undrained triaxial compression test characterised by $\dot{\varepsilon}_\mathrm{v} = 0$. An initial value of $\dot{p}_i = 0$ is expected, so that the stress path is perpendicular to the hydrostatic axis in principal stress space. This can be achieved with

$$\chi_{4i} = 0. \tag{18}$$

Factor χ_{2i} allows an independent calibration of directional stiffness in isotropic compression and undrained/drained shear, as discussed by Herle and Kolymbas [8]. In an isotropic compression test, Eq. 17a becomes

$$-\dot{p} = \frac{1}{3} f_\mathrm{s} \left(\hat{a}_i^2 + \frac{1}{3}\chi_{2i} \right) \dot{\varepsilon}_\mathrm{v} \triangleq K_i^+ \dot{\varepsilon}_\mathrm{v}. \tag{19}$$

where $K_i^+ = (1/3) f_\mathrm{s} (\hat{a}_i^2 + (1/3)\chi_{2i})$ represents the tangential bulk modulus of a soil. On the other hand, a shear test via triaxial compression is described by

$$-\dot{p} = \frac{1}{3} f_\mathrm{s} \left[\left(\hat{a}^2 + \frac{1}{3}\chi_2 \right) \dot{\varepsilon}_\mathrm{v} + \chi_2 \hat{q}\, \dot{\varepsilon}_\mathrm{q} + \hat{a}\, \chi_4 \sqrt{\frac{1}{3}\dot{\varepsilon}_\mathrm{v}^2 + \frac{3}{2}\dot{\varepsilon}_\mathrm{q}^2} \right], \tag{20a}$$

$$\dot{q} = f_\mathrm{s} \left[\frac{3}{2}\hat{a}^2 \dot{\varepsilon}_\mathrm{q} + \hat{q} \left(\frac{1}{3}\chi_2 \dot{\varepsilon}_\mathrm{v} + \chi_2 \hat{q} \dot{\varepsilon}_\mathrm{q} \right) + (1+\chi_4)\hat{a}\hat{q} \sqrt{\frac{1}{3}\dot{\varepsilon}_\mathrm{v}^2 + \frac{3}{2}\dot{\varepsilon}_\mathrm{q}^2} \right]. \tag{20b}$$

where q and $\dot{\varepsilon}_\mathrm{q}$ are defined in the same way as in [22]: $q = \sigma_\mathrm{a} - \sigma_\mathrm{r}$ and $\dot{\varepsilon}_\mathrm{q} = (2/3)(\dot{\varepsilon}_\mathrm{a} - \dot{\varepsilon}_\mathrm{r})$, and $\hat{q} = -(1/3)q/p = (\sigma_\mathrm{a} - \sigma_\mathrm{r})/(\sigma_\mathrm{a} + 2\sigma_\mathrm{r})$. In a drained shear test with constant mean pressure (isobaric shear), i.e. $\dot{p} \equiv 0$, we have initially $\dot{\varepsilon}_{\mathrm{v}i} = 0$. In an undrained shear test, we have $\dot{\varepsilon}_\mathrm{v} \equiv 0$ (isochoric shear). For both tests starting from an isotropic stress state, we have initially

$$\dot{q}_i = \dot{q}|_{\hat{q}=0} = \frac{3}{2} f_\mathrm{s} \hat{a}_i^2 \dot{\varepsilon}_\mathrm{q} \triangleq 3 G_i \dot{\varepsilon}_\mathrm{q}. \tag{21}$$

Here $G_i = (1/2) f_\mathrm{s}\, \hat{a}_i^2$ represents the initial tangential shear modulus at an isotropic stress state. The ratio of $r_i = K^+_i / G_i$ may be considered as a material constant [8]. Then χ_{2i} is related to r_i by

$$\chi_{2i} = 3\,\hat{a}_i^2\,((3/2) r_i - 1). \tag{22}$$

The quantity χ_{3i} is determined by considering unloading in an isotropic compression test. For this case, with the χ_3 term being activated, Eq. 14 becomes

$$-\dot{p} = \frac{1}{3} f_s \left(\hat{a}_i^2 + \frac{1}{3}\chi_{2i} + \frac{1}{3}\chi_{3i} \right) \dot{\varepsilon}_v \triangleq K_i^- \dot{\varepsilon}_v. \tag{23}$$

Let $K_i^+ / K_i^- = \kappa/\lambda$, which leads to a constitutive equation which is consistent with Eq. 9b. This condition provides

$$\chi_{3i} = (\lambda/\kappa - 1)(3\hat{a}_i^2 - \chi_{2i}) = \frac{9}{2}\hat{a}_i^2 r_i (\lambda/\kappa - 1). \tag{24}$$

To determine χ_2 and χ_4 at the steady flow state, we first impose the requirement that the volumetric deformation vanishes. For an elementary test with $\hat{\boldsymbol{\sigma}} : \dot{\boldsymbol{\varepsilon}} \geq 0$, the tensor $\boldsymbol{B} = -\mathbf{L}^{-1} : \boldsymbol{N}$ can be written as

$$\boldsymbol{B} = -\frac{1}{\hat{a}} \left(\frac{\chi_4 \hat{a}^2 - \chi_2 \|\hat{\boldsymbol{\sigma}}_d\|^2}{\hat{a}^2 + \chi_2 \|\hat{\boldsymbol{\sigma}}\|^2} \hat{\boldsymbol{\sigma}} + \hat{\boldsymbol{\sigma}}_d \right). \tag{25}$$

It is easy to check that conditions 6 and 3 are fulfilled with $\chi_{4f} = \chi_{2f} \triangleq \chi_f$. With a fixed interpolation (given below) for χ_2 and χ_4, it is found that the model behaviour under drained conditions is insensitive to χ_f. However, the undrained shear behaviour is strongly influenced by χ_f. A constant χ_2 (i.e. $\chi_f = \chi_{2i}$) will lead to a too stiff response. On the other hand, a higher value of $\chi_f = 1$ will lead to softening behaviour in an undrained shear test. To model a normally consolidated clay, χ_f should take a value of about 0.5. This value is used in our assessment of the model performance.

For an arbitrary stress state, other than an isotropic state or a steady flow state, the factors χ_2, χ_3 and χ_4 are determined using the following interpolations:

$$\begin{aligned} \chi_2 &= \chi_{2i} + \eta^2(\chi_f - \chi_{2i}), \\ \chi_3 &= \chi_{3i} = \text{const}, \\ \chi_4 &= \eta^n \chi_f. \end{aligned} \tag{26}$$

Here $0 \leq \eta = |\hat{\boldsymbol{\sigma}}_d|/\hat{a} \leq 1$ varies monotonically from 0 to 1 for a shear test starting from an isotropic state, and n is a further parameter introduced to scale the volumetric deformation (discussed below). For simplicity, the factor χ_3 is set to a constant and this will be checked against experimental data for unloading.

A geometrical illustration of the present model at an isotropic stress state is given by the response envelope shown in Fig. 3c. The solid ellipse and dashed ellipses represent the model response for a unit magnitude strain rate with and without the χ_3-term, respectively. The model responses to isotropic compression and isotropic unloading are represented by the quantities $\dot{\boldsymbol{\sigma}}_a$ and $\dot{\boldsymbol{\sigma}}_b$, with a ratio of $\|\dot{\boldsymbol{\sigma}}_a\|/\|\dot{\boldsymbol{\sigma}}_b\| = \kappa/\lambda$. The model response to isochoric shears is represented by the quantities $\dot{\boldsymbol{\sigma}}_c$ and $\dot{\boldsymbol{\sigma}}_d$, with $\|\dot{\boldsymbol{\sigma}}_c\| = \|\dot{\boldsymbol{\sigma}}_d\|$ and $\|\dot{\boldsymbol{\sigma}}_a\| / \|\dot{\boldsymbol{\sigma}}_c\| = f_s(\hat{a}_i^2 + (1/3)\chi_{2i})/f_s\hat{a}_i^2 = (3/2)K_i^+/G_i = (3/2)r_i$.

6. Shear-dilatancy behaviour of the model

In the interpolation 26 for the factor χ_4, a new parameter n has been introduced. With this new parameter, the volumetric deformation in shear tests can be scaled.

Consider a drained shear test via triaxial compression under constant mean pressure. By setting $\dot{p} = 0$ in Eq. 20a, a shear-dilatancy/contractancy relation is obtained for such a test:

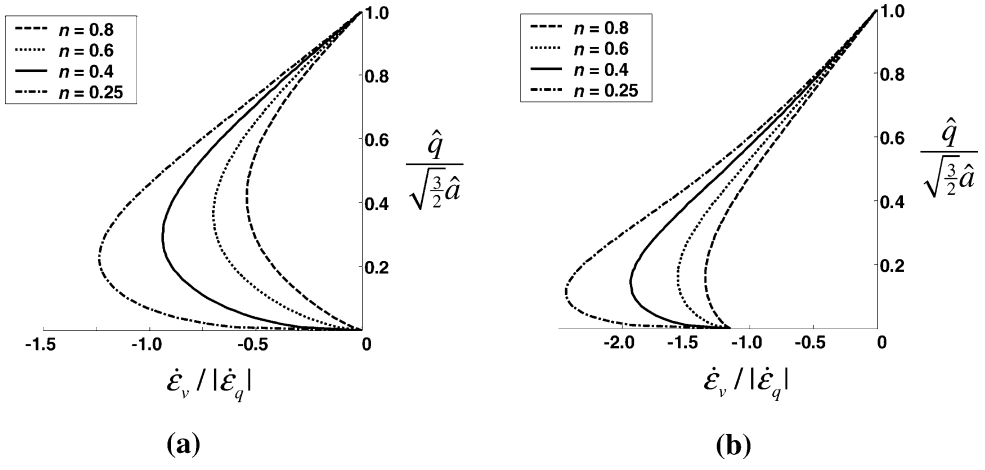

Fig. 4 Shear-dilatancy relation and its dependence on the parameter n for triaxial compression test **a** with constant mean pressure, and **b** with constant radial stress

$$\left(\hat{a}^2+\frac{1}{3}\chi_2\right)\dot{\varepsilon}_{\mathrm{v}}+\chi_2\hat{q}\dot{\varepsilon}_{\mathrm{q}}+\chi_4\hat{a}\sqrt{\frac{1}{3}\dot{\varepsilon}_{\mathrm{v}}^2+\frac{3}{2}\dot{\varepsilon}_{\mathrm{q}}^2}=0. \tag{27}$$

Equation 27 defines a nonlinear relation between the ratio of the strain rates $\dot{\varepsilon}_{\mathrm{v}}/|\dot{\varepsilon}_{\mathrm{q}}|$ and the normalized stress deviator $\hat{q}=-q/3p$. The dependence of this relation on the parameter n is shown in Fig. 4a. Note that we have $\dot{\varepsilon}_{\mathrm{v}}/|\dot{\varepsilon}_{\mathrm{q}}|=0$ at an isotropic state for $\hat{q}=0$ and χ_{4i}=0, and also at a steady flow state for $\hat{q}=\hat{q}_{\mathrm{f}}=\sqrt{(3/2)}\hat{a}_{\mathrm{c}}$ and $\hat{a}=\hat{a}_{\mathrm{c}}=\sqrt{(8/3)}\sin\varphi_{\mathrm{c}}/(3-\sin\varphi_{\mathrm{c}})$ under triaxial compression. These two stress points are independent of the parameter n, but the whole area under the $\hat{q}\sim\dot{\varepsilon}_{\mathrm{v}}/|\dot{\varepsilon}_{\mathrm{q}}|$ curve, which determines the total volume change in a constant pressure triaxial compression test, increases with a decreasing value of n.

Similarly, a shear-dilatancy/contractancy equation can be obtained for a drained triaxial compression test with a constant radial stress. In this case we have $\dot{q}=-3\dot{p}$, and Eq. 19 yields the following relation:

$$\left[\hat{a}^2+\frac{1}{3}\chi_2(1-\hat{q})\right]\dot{\varepsilon}_{\mathrm{v}}+\left(\chi_2\hat{q}-\frac{3}{2}\hat{a}^2-\chi_2\hat{q}^2\right)\dot{\varepsilon}_{\mathrm{q}}+[\chi_4-(1+\chi_4\hat{q})]\hat{a}\sqrt{\frac{1}{3}\dot{\varepsilon}_{\mathrm{v}}^2+\frac{3}{2}\dot{\varepsilon}_{\mathrm{q}}^2}=0. \tag{28}$$

Figure 4b shows the $\hat{q}\sim\dot{\varepsilon}_{\mathrm{v}}/|\dot{\varepsilon}_{\mathrm{q}}|$ response for this case and its dependence on the parameter n.

7. Model response to oedometer test

The oedometer test, also known as a K_0–consolidation test, is available in most soil testing laboratories and is often used to determine the consolidation behaviour of soils. In a standard oedometer test, the specimen is under proportional loading or unloading, which is characterised by $\dot{\varepsilon}_{\mathrm{a}}<0$ for loading and $\dot{\varepsilon}_{\mathrm{a}}>0$ for unloading and $\dot{\varepsilon}_{\mathrm{r}}=0$. It has been shown [9] that the stress rate response defined by the present type of constitutive model is proportional or nearly proportional, depending on the initial stress state. If the specimen is initially in a K_0-state, i.e. $\sigma_{\mathrm{r}}=K_0\sigma_{\mathrm{a}}$, the stress rate response is K_0 proportional so that $\dot{\sigma}_{\mathrm{r}}=K_0\dot{\sigma}_{\mathrm{a}}$. Otherwise, a K_0-state will be approached asymptotically. The value of K_0 for a normally consolidated clay, denoted as $K_{0\mathrm{nc}}$, can be predicted by the present model.

For a $K_{0\mathrm{nc}}$ state under 1D compression, Eq. 14 can be written as

$$\begin{aligned}\dot{\sigma}_{\mathrm{a}}&=f_{\mathrm{s}}[\hat{a}^2+\eta_2\hat{\sigma}_{\mathrm{a}}^2-\hat{a}(\chi_4+1)\hat{\sigma}_{\mathrm{a}}+\hat{a}/3]\dot{\varepsilon}_{\mathrm{a}},\\ \dot{\sigma}_{\mathrm{r}}&=f_{\mathrm{s}}[\eta_2\hat{\sigma}_{\mathrm{r}}^2-\hat{a}(\chi_4+1)\hat{\sigma}_{\mathrm{r}}+\hat{a}/3]\dot{\varepsilon}_{\mathrm{a}}.\end{aligned} \tag{29}$$

Noting the relations $\dot{\sigma}_{\mathrm{r}}/\dot{\sigma}_{\mathrm{a}}=\hat{\sigma}_{\mathrm{r}}/\hat{\sigma}_{\mathrm{a}}=\sigma_{\mathrm{r}}/\sigma_{\mathrm{a}}=K_{0\mathrm{nc}}$, the following relationship can be derived:

$$K_{0\mathrm{nc}}=\frac{1}{1+3\hat{a}}. \tag{30}$$

Using the representation for $\hat{a}$ in Eq. 7, an explicit relation between $K_{0\mathrm{nc}}$ and the critical friction angle φ_{c} can be obtained according to

$$K_{0\mathrm{nc}}=\frac{\sqrt{(6\hat{a}_i-1)^2+4(2+3\hat{a}_i)}-(6\hat{a}_i-1)}{2(2+3\hat{a}_i)}, \tag{31}$$

where $\hat{a}_i$ is defined by Eq. 8. The predicted dependence of $K_{0\mathrm{nc}}$ on the friction angle φ_{c} is presented in Fig. 5a, and may be compared with Jâky's empirical relation

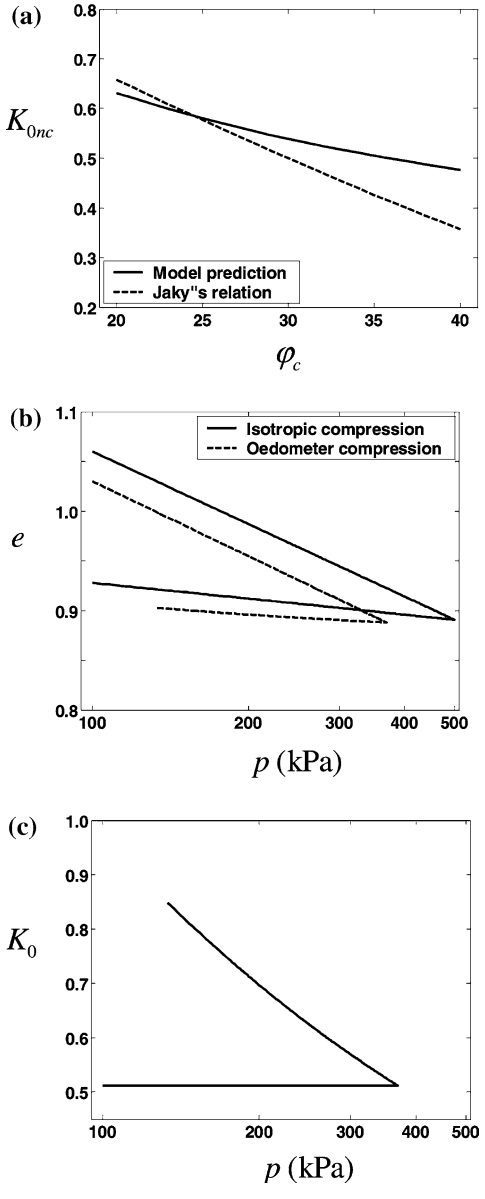

Fig. 5 Model response for oedometer test: **a** $K_{0\mathrm{nc}}-\varphi_{\mathrm{c}}$ relation, **b** e – log p relation and **c** variation of K_0 with mean pressure p

Table 1 Constitutive parameters for the Fujinomori clay

Present model	φ_c	λ	κ	r_i	n
	34°	0.1046	0.0231	0.867	0.4
Mašín's model	φ_c	λ^*	κ^*	r	N^*
	34°	0.0445	0.0108	1.3	0.8867

$$K_{0nc} = 1 - \sin\,\varphi_c. \tag{32}$$

The current model predicts a gradient for the $e - \ln p$ relation from an oedometer test which is different from the λ obtained from isotropic compression. Niemunis [16] noticed this possibility in previous hypoplastic formulations and introduced a factor in his visco-hypoplastic model to rectify this behaviour. The difference predicted by the present model, however, is rather small. Using the parameters given in Table 1, the predicted $e - \ln p$ curves for oedometer compression and unloading are shown in Fig. 5b, and may be compared with those for isotropic compression and unloading. For oedometer compression, the predicted gradient is slightly greater than λ, but the difference may be hard to detect from typical laboratory data. For oedometer unloading, however, the gradient of the $e - \ln p$ curve is smaller than κ, the corresponding gradient for isotropic unloading. This is due to the variation of K_0 during oedometer unloading. A quite realistic variation of K_0 is predicted by the present model (Fig. 5c).

8. Performance of the model

The proposed simple hypoplastic model contains five parameters; namely, λ, κ, φ_c, r_i and n. Here λ and κ are two dimensionless parameters, defining soil compressibility and swelling under isotropic compression and unloading, which are determined from an isotropic consolidation test. The parameter φ_c defines the shear strength at the critical state, while the parameters r_i and n are related to the shear stiffness and volumetric deformation in a shear test. These three parameters can be determined either from a triaxial compression tests with constant mean pressure or a conventional triaxial compression test.

To demonstrate the performance of the proposed model, the model responses are compared with experimental results for a remoulded clay—Fujinomori clay [13]—from conventional triaxial tests and true triaxial tests. The remoulded clay has a compression index of λ=0.1046, a swelling index of κ=0.0231, and a void ratio of e_0=1.06 at a mean pressure of p_0=49 kPa. The shear tests were started after an initial isotropic compression up to p=196 kPa. This isotropic state with e=0.915 is considered as the initial state for obtaining model predictions. The model responses under these loading conditions are obtained by numerical integration of the constitutive equations along the specified stress paths. The responses of the hypoplastic model

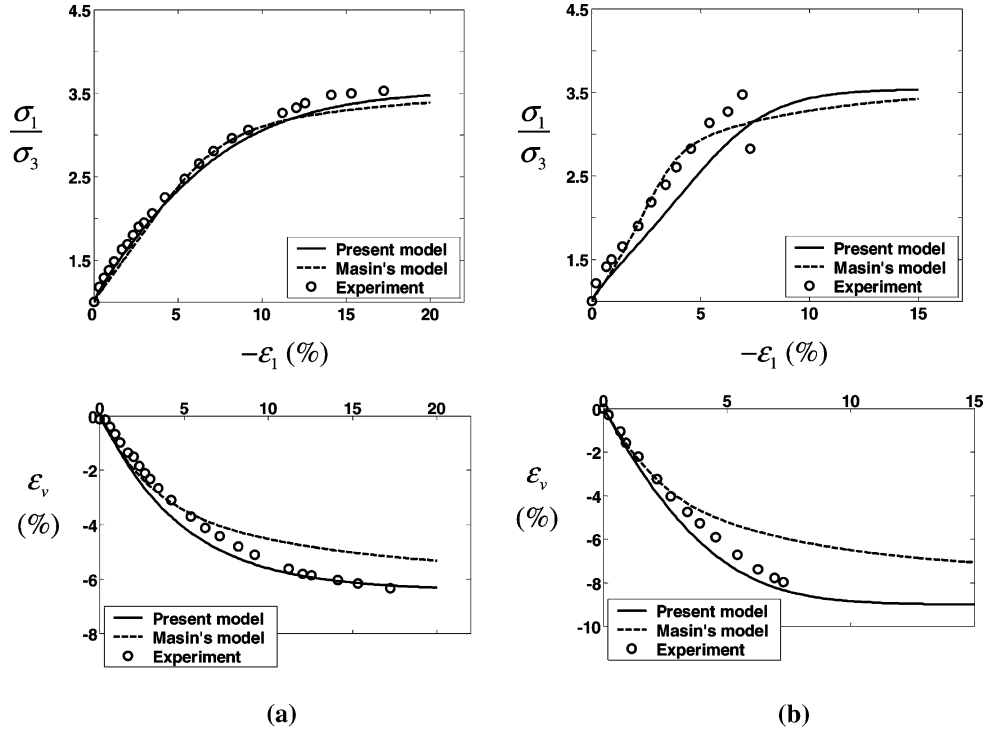

Fig. 6 Comparison of model predictions and experimental results for **a** triaxial compression and **b** triaxial extension

formulated by Mašín (2004) are also presented for a comparison. The parameters used for model predictions are listed in Table 1. The compression and swelling indexes are taken from Nakai et al. [13]. Other parameters are calibrated against the experimental data for triaxial compression test under constant mean pressure. Predictions are then made to compare with other test results.

Figure 6 presents the model predictions and experimental results for the Fujinomori clay under triaxial compression and extension with a constant stress component $\sigma_3 = -196\,\text{kPa}$. These results are shown in terms of the principal stress ratio and volumetric strain against the major principal strain. It can be seen that the response of the proposed model matches well the experimental data for the stress ratio and volumetric strain in both triaxial compression and triaxial extension. With the values for the parameters listed in Table 1, Mašín's model captures the stress ratio, but underestimates the volumetric strain. Decreasing parameter N^* will improve the volumetric strain predictions but worsen the stress ratio predictions.

Figure 7 compares the model predictions with the results from true triaxial tests, presented in terms of the principal stress ratio and the volumetric strain against the major principal strain. These results are for a constant mean pressure of p=196 kPa and various Lode angles θ of 0°, 15°, 30°, 45° and 60° in sequence. The experimental results for the stress ratio and volumetric strain are well matched by both the proposed model and Mašín's model. In some stress paths, however, Mašín's model shows a slight concavity in the stress-ratio strain curves.

A key issue in capturing soil behaviour is the accurate modelling of undrained loading. The proposed hypoplastic model is able to predict the undrained behaviour of normally consolidated clays. This capability is shown in Fig. 8, for an undrained triaxial compression test, and in Fig. 9 for an undrained triaxial extension test. The tests are started with an initial isotropic stress state of p_0=196 MPa. The total radial stress in the triaxial compression test is kept constant, while the total axial stress in the triaxial extension test is kept constant. We can see that the proposed model correctly predicts the effective stress path, as well as the variation of the axial and radial effective stresses with respect to the deviatoric strain, in these tests. In contrast, the predicted effective stress path predicted by Mašín's model deviates significantly from the experimental data. Moreover, an incorrect trend for the axial effective stress is predicted: the predicted axial effective stress first decreases and then increases, while the experimental data shows the reverse.

Finally, the model predictions for a loading–unloading sequence are presented in Figs. 10 and 11. The model predictions are compared with the experimental results of [14] for Fujinomori clay under cyclic loading. The experimental

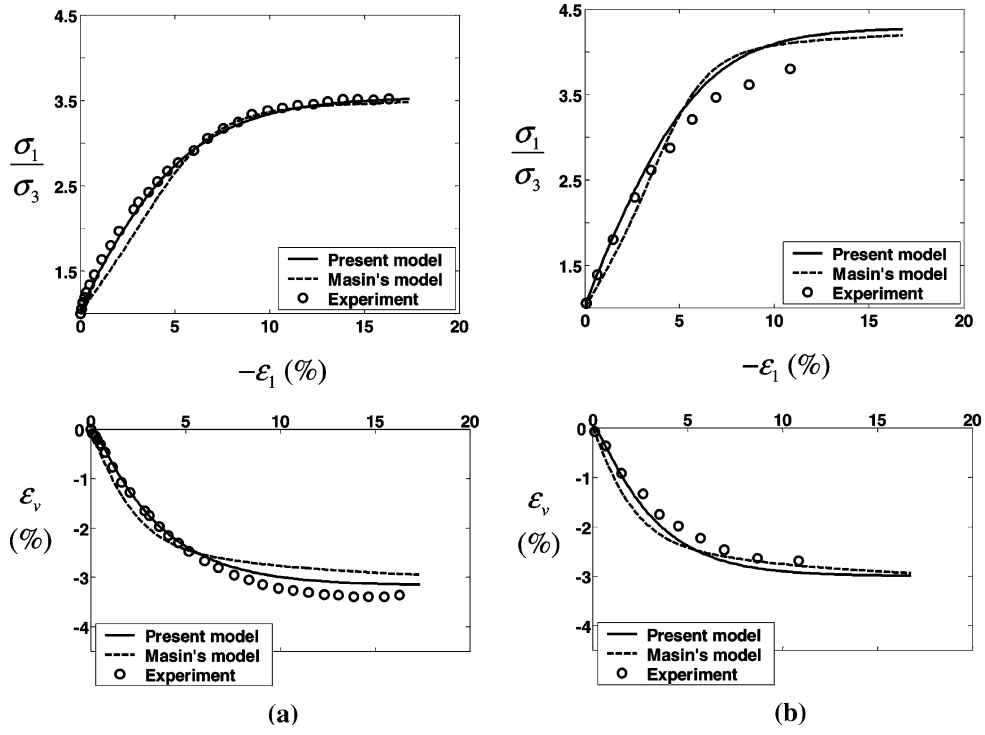

Fig. 7 Model predictions and experimental results for true triaxial tests with a constant mean pressure and a Lode angle of **a** θ=0°, **b** θ=15°, **c** θ=30°, **d** θ=45° and **e** θ=60°

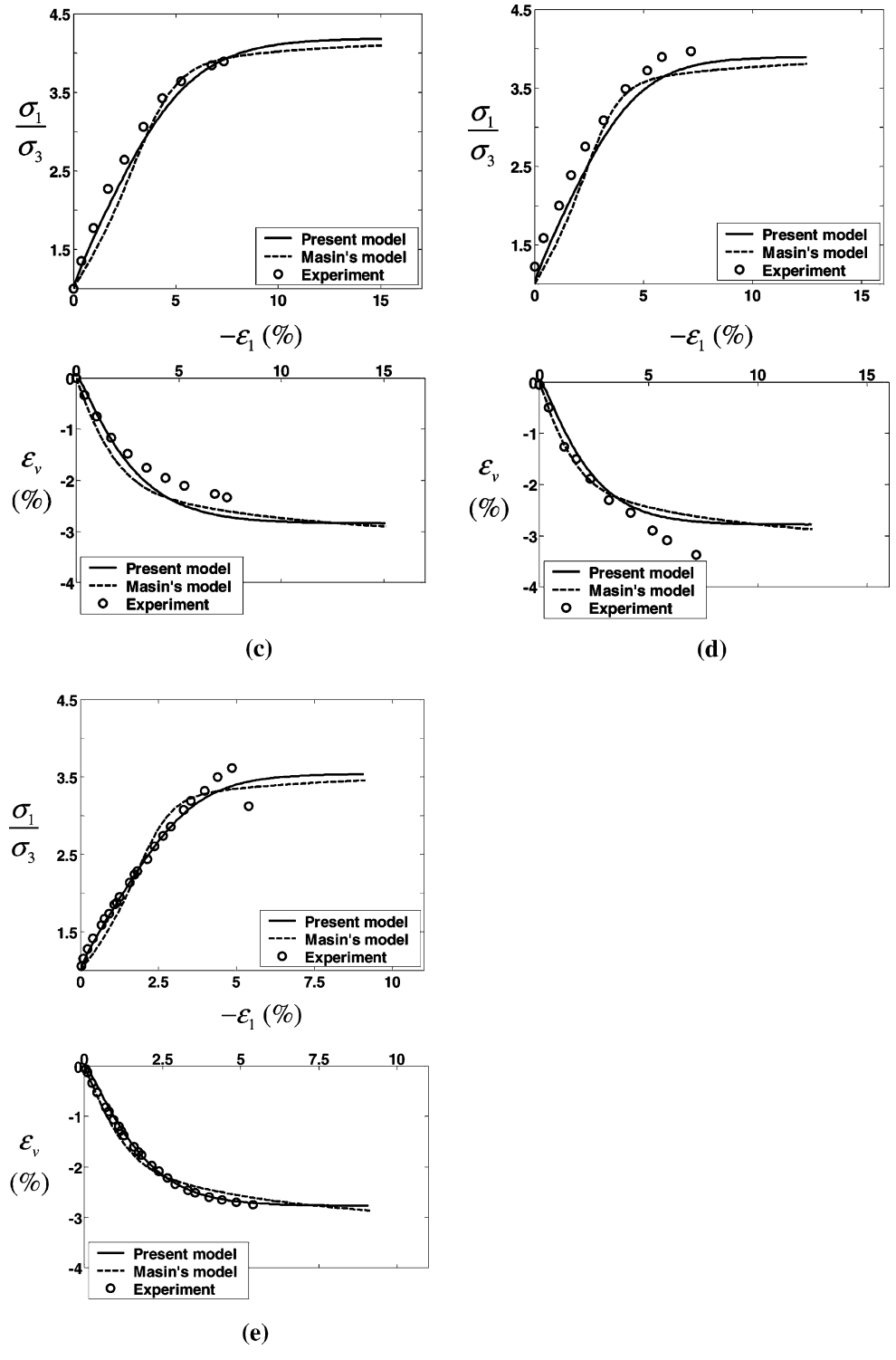

Fig. 7 continued

data for the first cycle of loading and unloading in a triaxial compression test, with constant radial stress and constant mean pressure, are taken for comparison. We note that although the same type of clay was used for these laboratory tests, the clay for the new tests [14] seems somewhat stiffer than that tested 18 years ago [13]. Using the same values for the soil parameters calibrated against the earlier test results (cf. Figs. 6, 7), the two models predict volumetric strains that are too large. Nevertheless, both constitutive models predict a reasonable response for unloading.

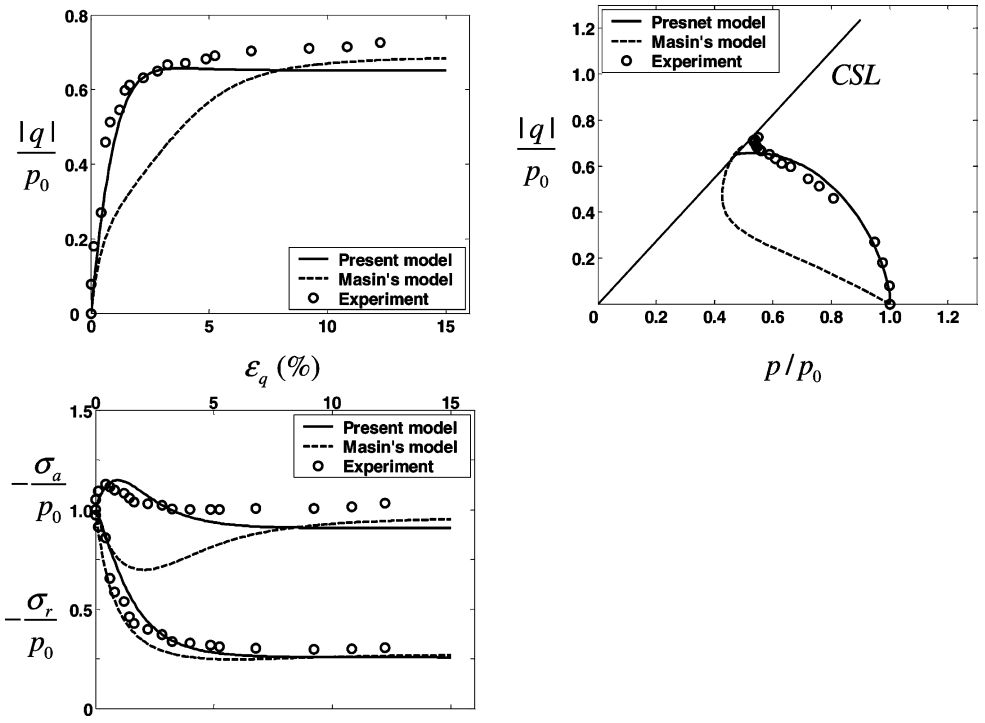

Fig. 8 Model predictions and experimental results for undrained triaxial compression test under constant total radial stress (p_0=196 MPa)

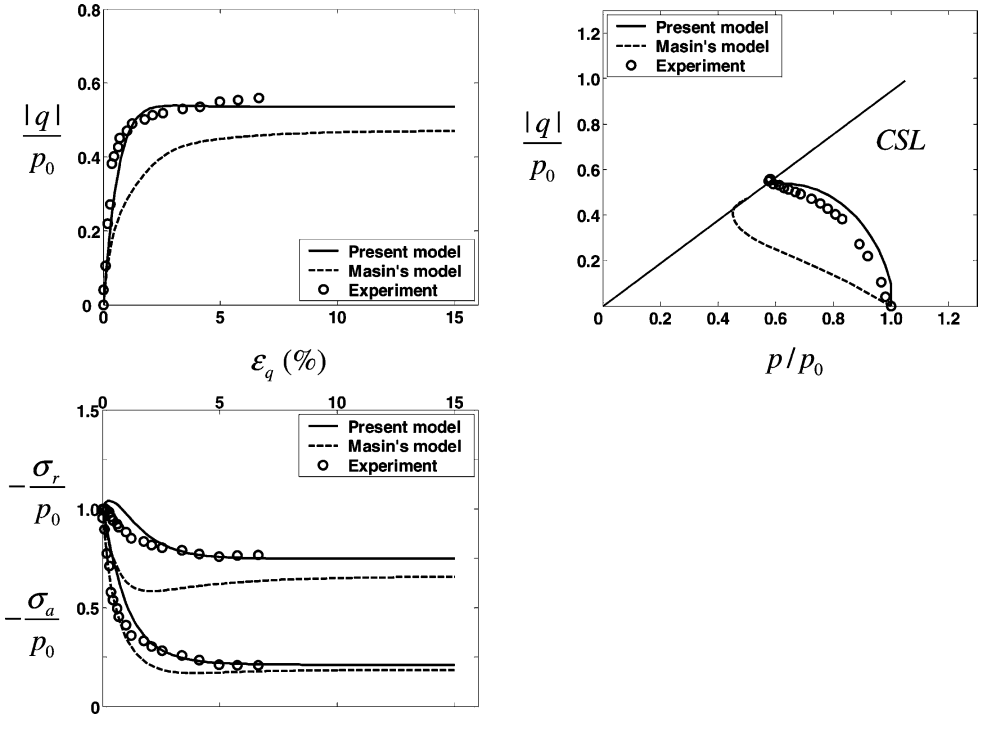

Fig. 9 Model predictions and experimental results for undrained triaxial extension test under constant total axial stress (p_0=196 MPa)

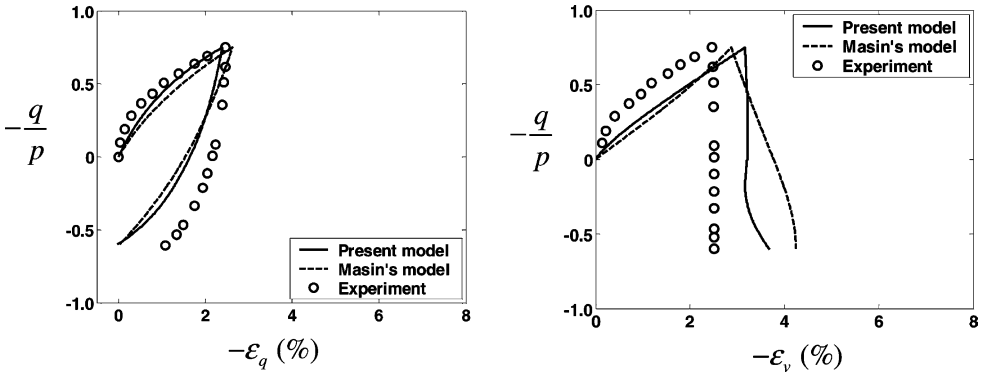

Fig. 10 Model predictions and experimental results for reverse loading in drained triaxial compression test under constant radial stress of 196 MPa

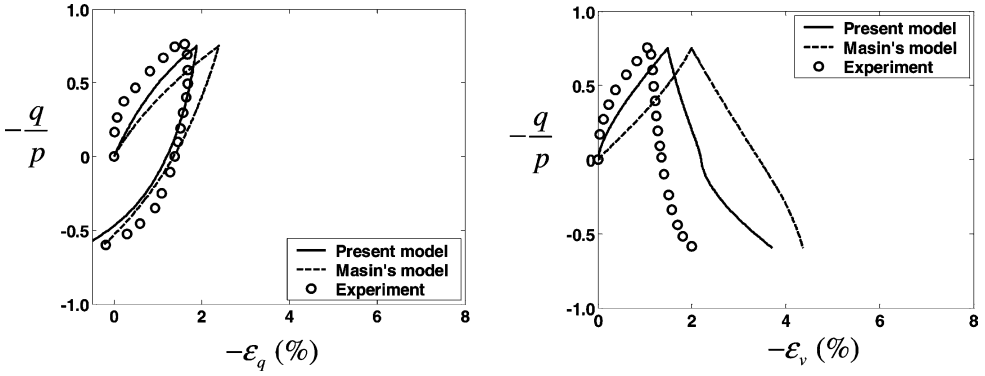

Fig. 11 Model predictions and experimental results for reverse loading in drained triaxial compression test under constant mean pressure of 196 MPa

9. Conclusion

A simple hypoplastic model for normally consolidated clay has been proposed in the light of a response envelope. The model is formulated by considering soil response under various stress paths in a true triaxial test. Special effort has been made to improve the model response for undrained loading. An explicit representation governing the shear-contractancy/dilatancy behaviour in a triaxial compression tests has been derived, which provides a better understanding of this type of model's ability to predict volumetric deformation. The model contains five constitutive constants, all of which can be easily determined from an isotropic consolidation test and a conventional drained triaxial compression test. The model can capture many key features of clay soil's response to loading and unloading, for medium to large strains under either drained or undrained conditions.

Acknowledgement The financial support of Australian Research Council (grant DP0453056) is gratefully acknowledged by the first author.

Appendix

Here we present a brief description of the hypoplastic model proposed by Mašín [12]. The constitutive equation is

$$\dot{\boldsymbol{\sigma}} = f_{\mathrm{s}}\,\mathbf{L} : \dot{\boldsymbol{\varepsilon}} + f_{\mathrm{s}} f_{\mathrm{d}} \boldsymbol{N} \|\dot{\boldsymbol{\varepsilon}}\| \,.$$

Here the fourth order tensor $\mathbf{L}$ takes the form

$$\mathbf{L} = 3(c_1\,\mathbf{I} + c_2 a^2 \hat{\boldsymbol{\sigma}} \otimes \hat{\boldsymbol{\sigma}}),$$

and the second order tensor $\boldsymbol{N}$ is given as

$$\boldsymbol{N} = \mathbf{L} : \left(-Y \frac{\boldsymbol{m}}{\|\boldsymbol{m}\|}\right),$$

with $\boldsymbol{m}$ being defined by

$$\boldsymbol{m} = -\frac{a}{F}\left[\frac{(F/a)^2 - \hat{\boldsymbol{\sigma}}_{\mathrm{d}} : \hat{\boldsymbol{\sigma}}_{\mathrm{d}}}{(F/a)^2 + \hat{\boldsymbol{\sigma}} : \hat{\boldsymbol{\sigma}}} \hat{\boldsymbol{\sigma}} + \hat{\boldsymbol{\sigma}}_{\mathrm{d}}\right].$$

In these equations, the parameters a and F are related to the critical friction angle φ_{c} and the Lode angle θ through the relation [21]

$$a = \frac{\sqrt{3}\,(3 - \sin\,\varphi_c)}{2\sqrt{2}\,\sin\,\varphi_c},$$

$$F = \sqrt{\frac{1}{8}\tan^2\psi + \frac{2 - \tan^2\psi}{2 + \sqrt{2}\tan\psi\cos(3\theta)}} - \frac{1}{2\sqrt{2}}\tan\psi$$

with $\tan\psi = \sqrt{3}|\hat{\boldsymbol{\sigma}}_d|$. The parameter Y in expression for $\boldsymbol{N}$, known as the degree of nonlinearity [16], has the following form:

$$Y = \left(\frac{\sqrt{3}a}{3 + a^2} - 1\right)\frac{(I_1I_2 + 9I_3)(1 - \sin^2\varphi_c)}{8I_3\sin^2\varphi_c} + \frac{\sqrt{3}a}{3 + a^2},$$

where I_1, I_2 and I_3 are the first, second and third stress invariants, respectively:

$$I_1 = \mathrm{tr}\boldsymbol{\sigma}, \quad I_2 = \frac{1}{2}[\boldsymbol{\sigma} : \boldsymbol{\sigma} - (I_1)^2], \quad I_3 = \det\boldsymbol{\sigma}.$$

The factors f_s and f_d in Eq. 29 are defined by

$$f_s = -\frac{\mathrm{tr}\boldsymbol{\sigma}}{\lambda^*}(3 + a^2 - 2^\alpha a\sqrt{3})^{-1},$$

$$f_d = \left[-\frac{1}{2}\mathrm{tr}\boldsymbol{\sigma}\exp\left(\frac{\log(1 + e) - N^*}{\boldsymbol{\lambda}^*}\right)\right]^\alpha,$$

where the scalar parameter α can be determined from

$$\alpha = \frac{1}{\ln 2}\ln\left[\frac{\lambda^* - \kappa^*}{\lambda^* + \kappa^*}\frac{3 + a}{\sqrt{3}a}\right].$$

The factors c_1 and c_2 in above equation are related to other parameters via

$$c_1 = \frac{2(3 + a^2 - 2^\alpha a\sqrt{3})}{9r}, \quad c_2 = 1 + (1 - c_1)\frac{3}{a^2}.$$

The model contains five parameters: φ_c, λ^*, κ^*, r and N^*, where φ_c is the critical state friction angle, λ^* and κ^* has the same meaning as in Eq.10a, b, r is the ratio of the bulk modulus over the shear modulus at an isotropic stress state, $r=K^+_i/G_i$, and N^* represents the logarithmic specific volume at a mean pressure of 1 kPa so that $N^*=\ln(1+e)|_{p=1\ \mathrm{kPa}}$.

References

1. Bauer E (1996) Calibration of a comprehensive hypoplastic model for granular materials. Soils Found 36(1):13–26
2. Bauer E (2000) Conditions for embedding Casagrade's critical states into hypoplasticity. Mech Cohes Frict Mater 5:125–148
3. Been K, Jefferies MG (1985) A state parameter for sands. Geotechnique 35(1):99–112
4. Butterfield R(1979) A natural compression law for soils. Geotechnique 29(4):469–480
5. Chambon R, Desrues J, Charlier R, Hammad W (1994). CLoE, a new rate type constitutive model for geomaterials: theoretical basis and implementation. Int J Numer Anal Methods Geomech 18(4):253–278
6. Gudehus G (1979) A comparison of some constitutive laws for soils under radially symmetric loading and unloading. In: Wittke (ed) Proceeds of the third international conference on numerical methods in geomechanics. A.A. Balkema, Aachen, pp 1309–1325.
7. Gudehus G (1996) A comprehensive constitutive equation for granular materials. Soils Found 36(1):1–12
8. Herle I, Kolymbas D (2004) Hypoplasticity for soils with low friction angles. Comput Geotech 31:365–373
9. Huang W (2000) Hypoplastic modelling of shear localization in granular materials. PhD Thesis, Graz University of Technology
10. Kolymbas D (2000) Introduction to hypoplasticity. A.A. Balkema, Rotterdam
11. Li XS, Dafalias YF (2000) Dilatancy for cohesionless soils. Geotechnique 50(4):449–460
12. Mašín D (2005) A hypoplastic constitutive model for clays. Int J Numer Anal Methods Geomech 29:311–336
13. Nakai T, Matsuoka H, Okuno N, Tsuzuki K (1986) True triaxial tests on normally consolidated clay and analysis of the observed shear behaviour using elastoplastic constitutive models. Soils Found 26(4):67–78
14. Nakai T, Hinokio M (2004) A simple elastoplastic model for normally and overconsolidated soils with unified materials parameters. Soils Found 44(2):53–70
15. Niemunis A, Herle I (1997) Hypoplastic model for cohesionless soils with elastic strain range. Mech Cohes Frict Mater 2(4):279–299
16. Niemunis A (2003) Extended hypoplastic model for soils. Schreftenreihe des Institutes für Grundbau und Bodenmechanik der Ruhr-Universität Bochum, Heft 34, Bochum
17. Roscoe KH, Schofield AN, Wroth P (1958) On the yielding of soils. Geotechnique 8:22–52
18. Schofield A, Wroth P (1968) Critical state soil mechanics. Cambridge University Press, Cambridge
19. Tamagnini C, Viggiani G, Chambon R (2000) A review of two different approaches to hypoplasticity. In: Kolymbas D (ed) Constitutive modelling of granular materials. Springer, Berlin Heidelberg New York, pp 107–165
20. Truesdell C (1955) Hypoplasticity. J Ration Mech Anal 4:83–133
21. von Wolffersdorff P-A (1996) A hypoplastic relation for granular materials with a predefined limit state surface. Mech Cohes Frict Mater 1:251–271
22. Wood DM (1990) Soil behaviour and critical state soil mechanics. Cambridge University Press, Cambridge
23. Wu W, Kolymbas D (1990) Numerical testing of the stability criterion for hypoplastic constitutive equations. Mech Mater 9:245–253
24. Wu W, Bauer E (1994) A simple hypoplastic constitutive model for sand. Int J Numer Anal Methods Geomech 18:833–862
25. Wu W, Niemunis A (1996) Failure criterion, flow rule and dissipation function derived from hypoplasticity. Mech Cohes Frict Mater 1:145–163
26. Wu W, Kolymbas D (2000) Hypoplasticity then and now. In: Kolymbas D (ed) Constitutive modelling of granular materials. Springer, Berlin Heidelberg New York, pp 57–105
27. Yao YP, Sun DA, Luo T (2004) A critical state model for sands dependent on stress and density. Int J Numer Anal Methods Geomech 28:323–337
28. Yu HS (1998) CASM: a unified state parameter model for clay and sand. Int J Numer Anal Methods Geomech 22:621–653